

Vortex Matter in Mesoscopic Superconducting Disks and Rings

F.M. Peeters [o], V.A. Schweigert [*], B.J. Baelus and P.S. Deo [†]

*Departement Natuurkunde, Universiteit Antwerpen (UIA),
Universiteitsplein 1, B-2610 Antwerpen, Belgium*

Abstract

Phase transitions between different (i.e. giant and multi-vortex) superconducting states and between the superconducting-normal state of mesoscopic disks and rings are studied in the presence of an external magnetic field by solving the two non-linear Ginzburg-Landau equations self-consistently. The flux through a circular disk with a hole in the middle is not quantized.

Key words: superconductivity, vortex, flux quantization

1 Introduction

Modern fabrication technology has made it possible to construct superconducting samples of micro- and submicrometer dimensions[1,2] which are comparable to the important length scales in the superconductor: the coherence (ξ) and the penetration length (λ). In such samples classical finite size effects are important which leads to flux confinement. The dimensions of the sample are considered to be sufficiently large such that quantum confinement of the single electron states are neglectable and the superconducting gap is not altered by the confinement. This is the regime in which the Ginzburg-Landau (GL) theory is expected to describe the superconducting state.

The size and shape of such samples strongly influences the superconducting properties. Whereas bulk superconductivity exists at low magnetic field (either the Meissner state for $H < H_{c1}$ in type-I and type-II superconductors or the Abrikosov vortex state for $H_{c1} < H < H_{c2}$ in type-II superconductors), surface superconductivity survives in infinitely large bounded samples up to the third critical field $H_{c3} \approx 1.695H_{c2}$ [3]. For mesoscopic samples of different shape, whose characteristic sizes are comparable to the coherence length ξ , recent experiments [1,2,4-6] have demonstrated the Little-Parks-type [7] oscillatory

behavior of the phase boundary between the normal and superconducting state in the $H - T$ plane, where T and H are the critical temperature and the applied magnetic field, respectively.

In the present paper we study superconducting disks of finite height with a hole in the center. Previous calculations were mainly concentrated on circular infinite long superconducting wires and hollow cylinders. In this case there are no demagnetization effects. Superconducting disks and rings of finite thickness have been studied much less extensively theoretically although they may often correspond more closely to experimental fabricated systems.

The giant vortex state in cylinders was studied in Ref. [8] and in Ref. [9] for infinitely thin disks and rings. Recently, Venegas and Sardella [10] used the London theory to study the vortex configurations in a cylinder for up to 18 vortices. They found that those vortices form a ring structure very similar to classical confined charged particles [11]. These results are analogous to those of Refs. [12,13] where the image method was used to determine the vortex configuration. The transition from the giant vortex to the multi-vortex state in a thin superconducting disk was studied in Ref. [14]. Square-shaped loops were investigated by Fomin *et al* [15] in order to explain the Little-Park oscillations found by Moshchalkov *et al* [1] and to study the effect of leads. In this case the magnetic field was taken uniform along the z -direction and demagnetization effects were disregarded. Loops of non zero width were studied by Bruyndoncx *et al* [16] within the linearized GL theory. The magnetic field was taken uniform and equal to the applied field which is valid for very thin rings. They studied the $T_c(H)$ phase boundary and in particular the 2D-3D dimensional cross over regime. A superconducting film with a circular hole was studied by Bezryadin *et al* [17]. This is the limiting case of the current ring structure for wide rings. Or conversely, it is the antidot version of the disk system studied in Refs. [2,18].

Most of previous calculations are restricted to the London limit (i.e. extreme type-II systems) or do not consider the demagnetization effect. Our approach is not limited to such situations and we calculate the superconducting wavefunction and the magnetic field fully self-consistently for a finite 3D system, i.e. for a disk and ring with finite width and thickness. The details of our numerical approach can be found in Ref. [19] and therefore will not be repeated. Here we investigate the flux expulsion in the Meissner state, the giant \rightarrow multi-vortex transition in fat rings, and the absence of flux quantization in rings of finite height and non zero width. In contrast to most of earlier work (see e.g. [16]) we are interested in the superconducting state deep inside the $T_c(H)$ phase diagram where the magnetic field in and around the superconductor is no longer homogeneous. The transition from disk to thin loop structures is also investigated.

2 Meissner state

Meissner and Ochsenfeld (1933) found that if a superconductor is cooled in a magnetic field to below the transition temperature, then at the transition the lines of induction are pushed out. The Meissner effect shows that a bulk superconductor behaves as if inside the specimen the magnetic field is zero, and consequently it is an ideal diamagnet. The magnetization is $M = -H_{\text{applied}}/4\pi$. This result is shown by the dashed curve in Fig. 1 which refers to the right axis.

Recently, Geim *et al* [2] investigated superconducting disks of different sizes. Fig. 1 shows the experimental results (symbols) for an Al disk of radius $R \sim 0.5\mu\text{m}$ and thickness $d \sim 0.15\mu\text{m}$. Our numerical results which includes a full self-consistent solution of the two non-linear GL equations are given by the solid curve but which refers to the right axis (we took $\lambda(0) = 0.07\mu\text{m}$, $\xi(0) = 0.25\mu\text{m}$ and $\kappa = 0.28$). There is very good qualitative agreement but quantitatively the theoretical results differ by a factor of 50.5. The latter can be understood as due to a detector effect. Experimentally the magnetization is measured using a Hall bar. Consequently, the magnetic field is averaged over the Hall cross and it is the magnetization resulting from the field expelled from this Hall cross which is plotted while theoretically we plotted the magnetization resulting from the field expelled from the disk. This is illustrated in Fig. 2 where we show a contour plot of the magnetic field profile in the plane of the middle of the disk and a cut through it (see inset of Fig. 2). The results are for a disk of radius $R = 0.8\mu\text{m}$ for a magnetic field such that $L = 5$ which implies that a giant vortex with six flux quanta is centered in the middle of the disk leading to an enhanced magnetic field near the center of the disk and expulsion of the field in a ring-like region near the edge of the sample. The demagnetization effect is clearly visible which leads to a strong enhancement of the field near the outer boundary of the disk. The theoretical result in Fig. 1 corresponds to an averaging of the magnetic field over the disk region while the Hall detector averages the field over a much larger area which brings the average field much closer to the applied field. The inset of Fig. 2 shows clearly regions with $H < H_{\text{applied}}$ which correspond to diamagnetic response and regions with $H > H_{\text{applied}}$ which correspond to paramagnetic response. The averaging over the detector area (if width of the detector $W > R$) adds additional averaging over paramagnetic regions to the detector output.

Using a Hall bar of width $W = 2.5\mu\text{m}$ a distance $h = 0.15\mu\text{m}$ separated from the superconducting disk results into an expelled field which is a factor 50.44 smaller than the expelled field of the disk and brings our theoretical results in Fig. 1 in quantitative agreement with the experimental results. This averaging over the Hall cross scales the results but does not change the shape of the curve as long as L is kept fixed. For different L this scale factor is slightly different

because it leads to different magnetic field distributions.

Notice also that the magnetization as function of the magnetic field is linear only over a small magnetic field range, i.e. $H < 20G$ and the slope (see dashed curve in Fig. 1) is a factor 2.5 smaller than expected from an ideal diamagnet. This clearly indicates that for such small and thin disks there is a substantial penetration of the magnetic field into the disk. This is illustrated in Fig. 3 where the magnetic field lines are shown for a superconducting disk of radius $R = 0.8\mu\text{m}$ in the $L = 0$ state, i.e. the Meissner state. This strong penetration of the magnetic field inside the disk is also responsible for the highly nonlinear magnetization curve for $H \gg 20G$.

3 Giant-vortex state versus multi-vortex state

Next, we generalize our system to a disk with thickness d and radius R_o containing a hole in the center with radius R_i . The system under consideration is circular symmetric and therefore if the GL equations would have been linear the Cooper pair wavefunction could have been written as $\Psi(\vec{\rho}) = F(\rho) \exp(iL\phi)$. We found that even for the nonlinear problem such a circular symmetric state, also called giant vortex state, still has the lowest energy when the confinement effects are dominant. This is the case when R_o is small or $R_o/R_i \approx 1$, or in the case of large magnetic fields when there is only surface superconductivity. This is illustrated in the phase diagram shown in Fig. 4 for a thin superconducting ring of outer radius $R_o/\xi = 4$ and width $R_o - R_i$. The equilibrium regions for the giant vortex states with different angular momentum L are separated by the solid curves. Notice that with decreasing width, i.e. increasing inner radius R_i : 1) the superconducting state survives up to large magnetic fields. This is a consequence of the enhanced superconductivity due to surface superconductivity which in the limit of $R_i \rightarrow R_o$ leads to $H_{c3} \rightarrow \infty$ [20]. 2) The L-transitions occur for $\Phi = (L + 1/2)\Phi_o$ in the limit $R_i \rightarrow R_o$, where $\Phi_o = hc/2e$ is the flux quantum.

For large type-II systems one expects the giant-vortex state to break up into the Abrikosov triangular lattice of single vortices. The nonlinear term in the GL theory is responsible for this symmetry breaking. Such a multi-vortex state is the lowest energy state for the shaded areas in Fig. 4. Notice that as compared to the disk case the presence of the hole in the center stabilizes the multi-vortex state. Except for large R_i because then the confinement effect starts to dominate which imposes the symmetry of the edge of the system on the superconducting state. Near the normal/superconducting boundary only surface superconductivity survives and the symmetry of the superconducting state is determined by the symmetry of the surface which leads to the giant vortex state. The same holds for the Meissner state (i.e. $L = 0$). For $L = 1$

there is one flux quantum in the center of the system and there is no distinction between the giant and the multi-vortex states. Only for $L \geq 2$ we can have broken symmetry configurations.

The transition from the multi-vortex state to the giant-vortex state with increasing magnetic field is illustrated in Fig. 5 where we plot the superconducting electron density for a disk with radius $R_o/\xi = 4$ containing a hole in the center with radius $R_i/\xi = 0.4$ and for a magnetic field range such that the vorticity is $L = 4$. First, we can clearly discriminate three vortices arranged in a triangle with one vortex in the center piercing through the hole (solid circle) of the disk. Increasing the magnetic field drives the vortices closer to the center and the single vortices start to overlap. Finally, for sufficiently large magnetic fields the four vortices form one circular symmetric giant-vortex state with winding number $L = 4$.

If the hole is sufficiently large more than one flux quantum can pierce through this hole for sufficiently large magnetic fields. This is illustrated in Fig. 6 for a ring of $R_o/\xi = 4, R_i/\xi = 1$ with an external magnetic field such that the vorticity is $L = 5$. There are four vortices in the superconducting material arranged on the edge of a square and two piercing through the hole. The latter conclusion can be easily verified by considering a contour plot of the phase (right contour plot in Fig. 6). Notice that encircling the hole the phase of the superconducting wavefunction changes with $2 \times 2\pi$ while encircling the outer edge of the ring it changes with $6 \times 2\pi$. In this plot the location of the vortices is also clearly visible. Encircling a single vortex changes the phase by 2π .

4 Is the flux through the hole of the ring quantized?

It is often mentioned that the flux through a loop is quantized into integer multiples of the flux quantum $\Phi_o = hc/2e$. In order to check the validity of this assertion we plot in Fig. 7(a) the flux through the hole of a wide ring of thickness $d/\xi = 0.1$ with outer $R_o/\xi = 2$ and inner radius $R_i/\xi = 1$. From this figure it is clear that the flux through the hole of such a ring is not quantized. Note that depending on the magnetic field strength there is compression or expulsion of magnetic field in the hole region (compare solid curve with dashed line which represents the flux $\Phi = \pi R_i^2 H$). The absence of quantization was also found earlier [21] for hollow cylinders when the thickness of the cylinder wall is smaller than the penetration length of the magnetic field. In order to understand this apparent breakdown of flux quantization lets turn to the derivation of the flux quantization condition. Inserting the wavefunction $\Psi = |\Psi| \exp(i\phi)$ into the current operator we obtain (under the assumption

that the spatial variation of the superconducting density is weak)

$$\vec{j} = \frac{e\hbar}{m} |\Psi|^2 (\vec{\nabla} \phi - \frac{2e}{\hbar c} \vec{A}), \quad (1)$$

which after integrating over a closed contour C inside the superconductor leads to

$$\oint_C \left(\frac{mc}{2e^2|\Psi|^2} \vec{j} - \vec{A} \right) \cdot d\vec{l} = L\Phi_o. \quad (2)$$

When the contour C is chosen along a path such that the superconducting current is zero we obtain

$$L\Phi_o = \oint_C \vec{A} \cdot d\vec{l} = \int \text{rot} \vec{A} \cdot d\vec{S} = \int \vec{H} \cdot d\vec{S} = \Phi, \quad (3)$$

which tells us that the flux through the area encircled by C is quantized. In our wide superconducting ring the current is non zero at the inner boundary of the ring and consequently the flux through the hole does not have to be quantized. In fact the flux will be $\Phi = L\Phi_o + \Phi_j$ where

$$\Phi_j = \Phi_o \frac{m}{he} \oint_C \frac{\vec{j}}{|\Psi|^2} \cdot d\vec{l}, \quad (4)$$

which depends on the size of the current at the surface of the inner ring.

The radius of the considered ring in Fig. 7 is sufficiently small that we have a circular symmetric vortex state and consequently the current has only an azimuthal component. The radial variation of this current is plotted in Fig. 8(a) for three different values of the winding number L for a fixed magnetic field. For $L \neq 0$ the current in such a wide ring reaches zero at some radial position ρ^* . As shown in Fig. 8(b) the corresponding flux through a surface with radius ρ^* is exactly quantized into $L\Phi_o$ as required by the above quantization condition. The current at the inner edge of the ring is clearly non zero and therefore it is easy to understand why the flux through the hole is not an integer multiple of the flux quantum. The effective radius ρ^* is plotted in Fig. 7(b) which is an oscillating function of the magnetic field. The dashed curves in the figure correspond to the values for the metastable states. Notice that ρ^* oscillates around the value $\sqrt{R_o R_i} = \sqrt{2} = 1.41$ which can be obtained within the London theory [22]. At the $L \rightarrow L + 1$ transition this radius exhibits a jump which moves closer towards the outer radius while for fixed L the effective radius becomes closer to the inner radius with increasing H .

Next we consider the magnetic field range, ΔH , needed to increase L with one flux quantum, i.e. it is the distance between two consecutive jumps in the magnetization. The corresponding flux $\Delta\phi = \pi R_o^2 \Delta H$ is shown in Fig. 9. For small R_o (see Fig. 9(a)) this value is almost independent of L for fixed R_i . Its value is approximately given by the flux increase with one flux quantum through a circular area with radius $\sqrt{R_o R_i}$ (dashed horizontal curves in Fig. 9). For larger R_o (see Fig. 9(b)) this relation is much more complicated and the distance between the jumps in the magnetic field is a strong function of L , except for $R_i \sim R_o$ where it is again determined by the flux quantization through an area with radius $\rho^* = \sqrt{R_i R_o}$.

5 Conclusion

Mesoscopic superconducting disks of non zero thickness containing a hole in the center were studied theoretically by solving numerically the coupled non linear GL equations. In thin structures there is a substantial penetration of the magnetic field into the superconductor leading to a large (non linear) demagnetization effect. The hole in the disk enhances superconductivity and for small holes it stabilizes the multi-vortex state. The flux through the hole of the disk is not quantized. But for rings with a narrow width an increase of the applied magnetic field with one flux quantum through a region with radius $\sqrt{R_i R_o}$ increases the winding number L with one unit.

Acknowledgement We acknowledge discussions with A. Geim and V. Moshchalkov. This work was supported by the Flemish Science Foundation (FWO-Vl) and IUAP-VI. FMP is a research director with the FWO-Vl.

References

- [o] Electronic address: peeters@uia.ua.ac.be.
- [*] Permanent address: Institute of Theoretical and Applied Mechanics, Russian Academy of Sciences, Novosibirsk 630090, Russia.
- [†] Present address: Department of Physics, University of Jyväskylä, P.O. box 35, 40351 Jyväskylä, Finland.
- [1] V.V. Moshchalkov, L. Gielen, C. Strunk, R. Jonckheere, X.Qui, C. Van Haesendonck, and Y. Bruynseraede, *Nature (London)* **373**, 319 (1995).
- [2] A.K. Geim, I.V. Grigorieva, S.V. Dubonos, J.G.S. Lok, J.C. Maan, A.E. Filippov, and F.M. Peeters, *Nature (London)* **390**, 259 (1997).
- [3] D. Saint-James and P.G. de Gennes, *Phys. Lett.* **7**, 306 (1963).

- [4] O. Buisson, P. Gandit, R. Rammal, Y.Y. Wang and B. Pannetier, Phys. Lett. **150**, 36 (1990).
- [5] C. Strunk, V. Bruyndoncx, V.V. Moshchalkov, C. Van Haesendonck, and Y. Bruynsraede, Phys. Rev. B **54**, R12701 (1996).
- [6] X. Zhang and J.C. Price, Phys. Rev. B **55**, 3128 (1997).
- [7] W.A. Little and R.D. Parks, Phys. Rev. Lett. **9**, 9 (1962).
- [8] V.V. Moshchalkov, X.G. Qiu, and V. Bruyndoncx, Phys. Rev. B **55**, 11793 (1997).
- [9] R. Benoist and W. Zwerger, Z. Phys. B **103**, 377 (1997).
- [10] P.A. Venegas and E. Sardella, Phys. Rev. B **58**, 5789 (1998).
- [11] V.M. Bedanov and F.M. Peeters, Phys. Rev. B **49**, 2667 (1994).
- [12] A.I. Buzdin and J.P. Brison, Phys. Lett. A **196**, 267 (1994).
- [13] S.H. Brongersma, E. Verweji, N.J. Koeman, D.G. de Groot, R. Griessen, and B.I. Ivlev, Phys. Rev. Lett. **71**, 2319 (1993).
- [14] V.A. Schweigert, F.M. Peeters, and P.S. Deo, Phys. Rev. Lett. **81**, 2783 (1998).
- [15] V.M. Fomin, V.R. Misko, J.T. Devreese, and V.V. Moshchalkov, Phys. Rev. B **58**, 11703 (1998).
- [16] V. Bruyndoncx, L. Van Look, M. Verschueren, and V.V. Moshchalkov, Phys. Rev. B **60**, 10468 (1999).
- [17] A. Bezryadin, A. Buzdin, and B. Pannetier, Phys. Rev. B **51**, 3718 (1995).
- [18] P.S. Deo, V.A. Schweigert, F.M. Peeters, and A.K. Geim, Phys. Rev. Lett. **79**, 4653 (1997).
- [19] V.A. Schweigert and F.M. Peeters, Phys. Rev. B **57**, 13817 (1998).
- [20] V.A. Schweigert and F.M. Peeters, Phys. Rev. B **60**, 3084 (1999). V.M. Fomin, J.T. Devreese, and V.V. Moshchalkov, Europhys. Lett. **42**, 553 (1998), *ibid.* **46**, 118 (1999).
- [21] R.P. Groff and R.D. Parks, Phys. Rev. **176**, 567 (1968).
- [22] G.F. Zharkov, in *Superconductivity, superdiamagnetism, superfluidity*, Ed. V.L. Ginzburg (MIR publishers, Moscow, 1987), p.126.

Fig. 1. Magnetization of an Al disk with radius $R = 0.44\mu m$ as function of the applied magnetic field. The symbols are the experimental results and the solid curve is our theoretical result.

Fig. 2. The magnetic field distribution in the horizontal plane through the middle of the superconducting disk with radius $R = 0.8\mu m$ for $L = 6$. The inset gives the magnetic field profile along the radial direction.

Fig. 3. The magnetic field distribution in and around a superconducting disk with radius $R = 0.8\mu m$ and thickness $d = 0.15\mu m$. The superconductor is in the Meissner state, i.e. $L = 0$.

Fig. 4. Phase diagram for the superconducting state of a ring of outer radius $R_o/\xi = 4$ as function of the inner radius R_i . The transition between states with different vorticity L is given by the solid curves. The region where the multi-vortex state has the lowest energy is shown by the shaded area. The thick solid curve gives the normal/superconducting phase boundary.

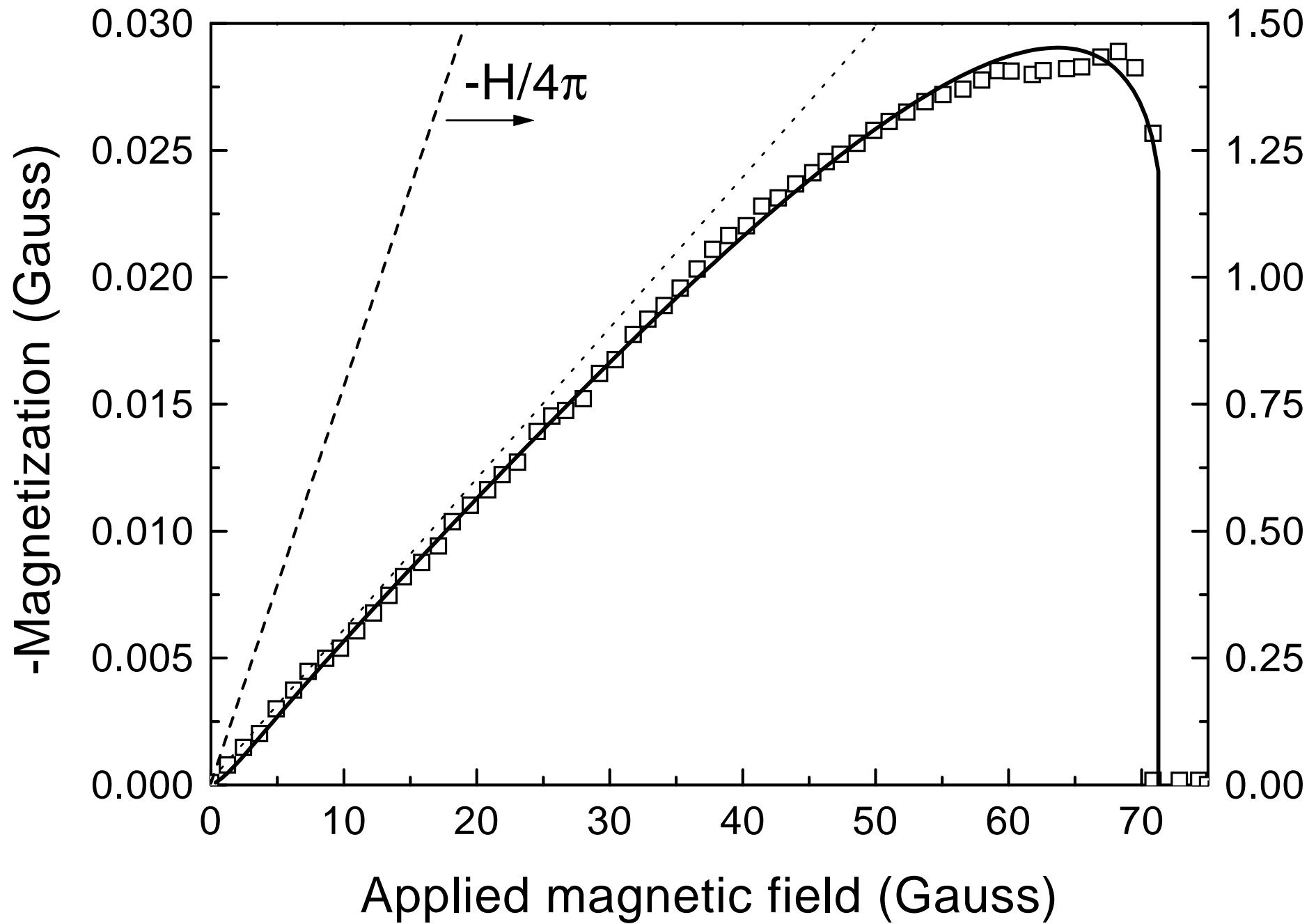
Fig. 5. The Cooper pair density for a ring with $R_o/\xi = 4$ and $R_i/\xi = 0.4$ for $H/H_{c2} = 0.72(1), 0.795(2), 0.87(3), 0.945(4)$.

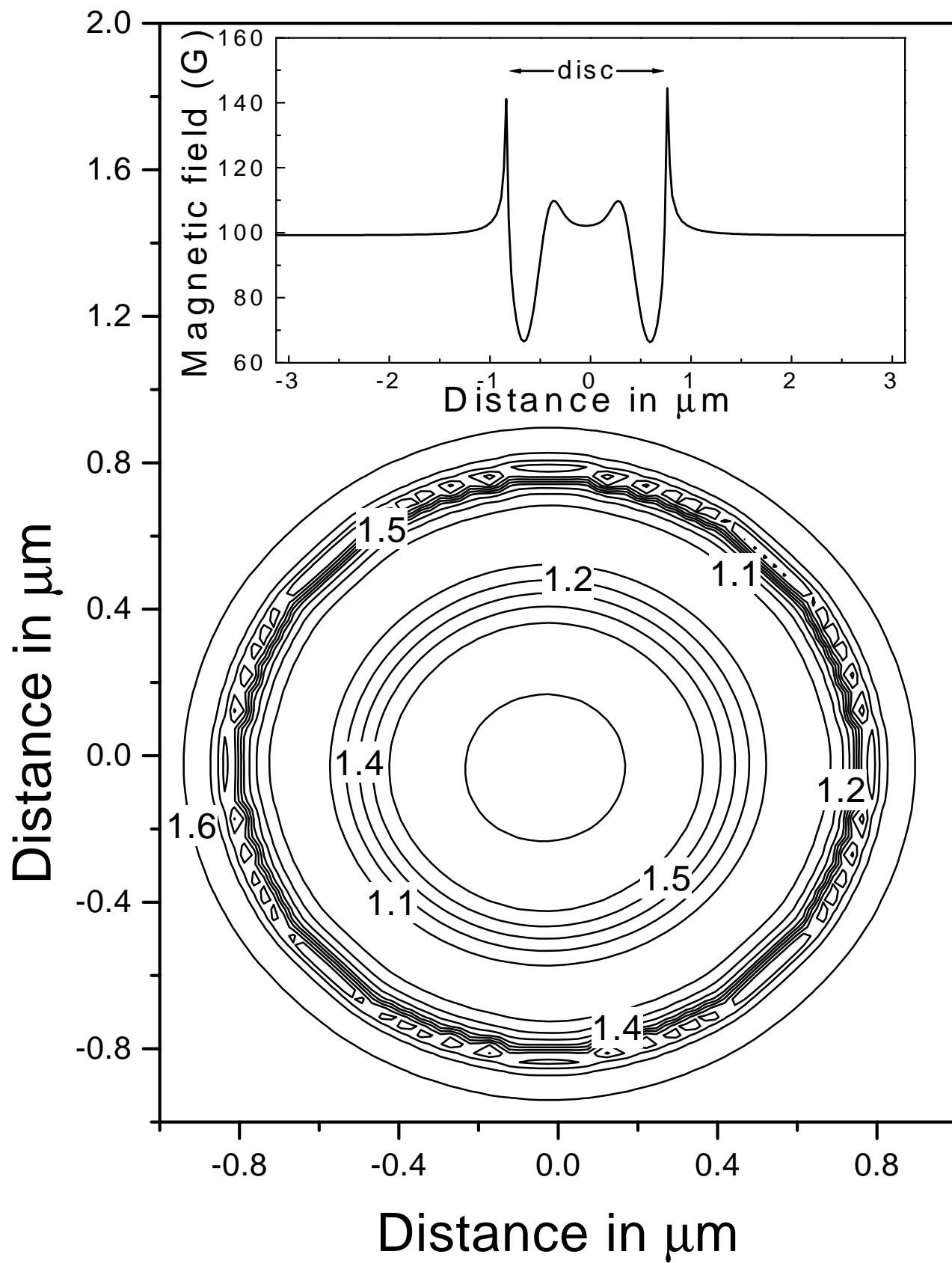
Fig. 6. The magnetic field distribution and a contour plot of the phase of the superconducting wavefunction for a ring with $R_o/\xi = 4$, $R_i/\xi = 1$ and $d/\xi = 0.005$ in the presence of an external magnetic field of $H/H_{c2} = 1.145$.

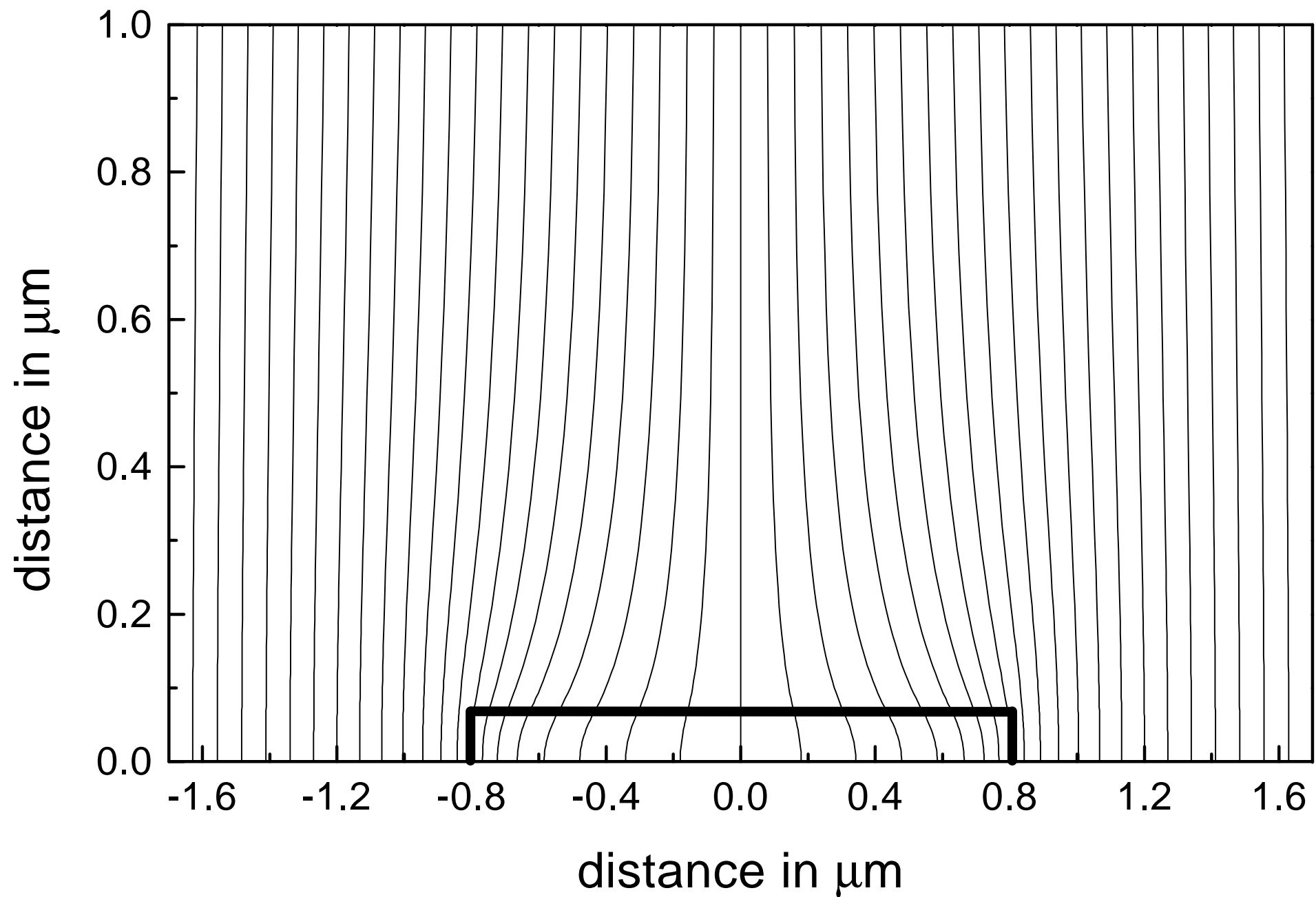
Fig. 7. (a) The flux through the hole of a ring with $R_o = 2\mu m$ and $R_i = 1\mu m$ as function of the magnetic field. (b) The effective radius for the circular surface area through which flux is quantized.

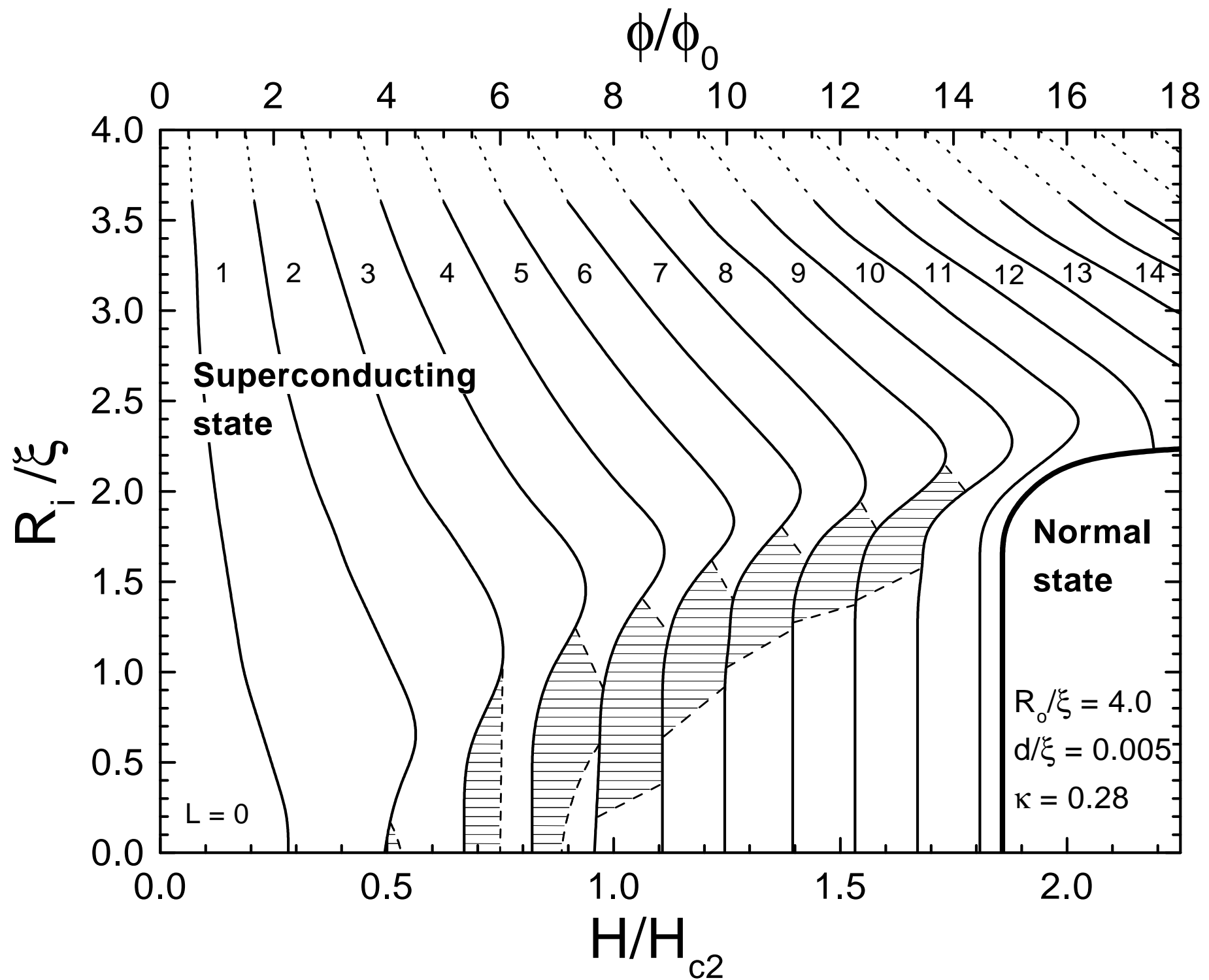
Fig. 8. (a) The radial dependence of the superconducting current through the ring of Fig. 7 and (b) the corresponding flux through the area with radius ρ .

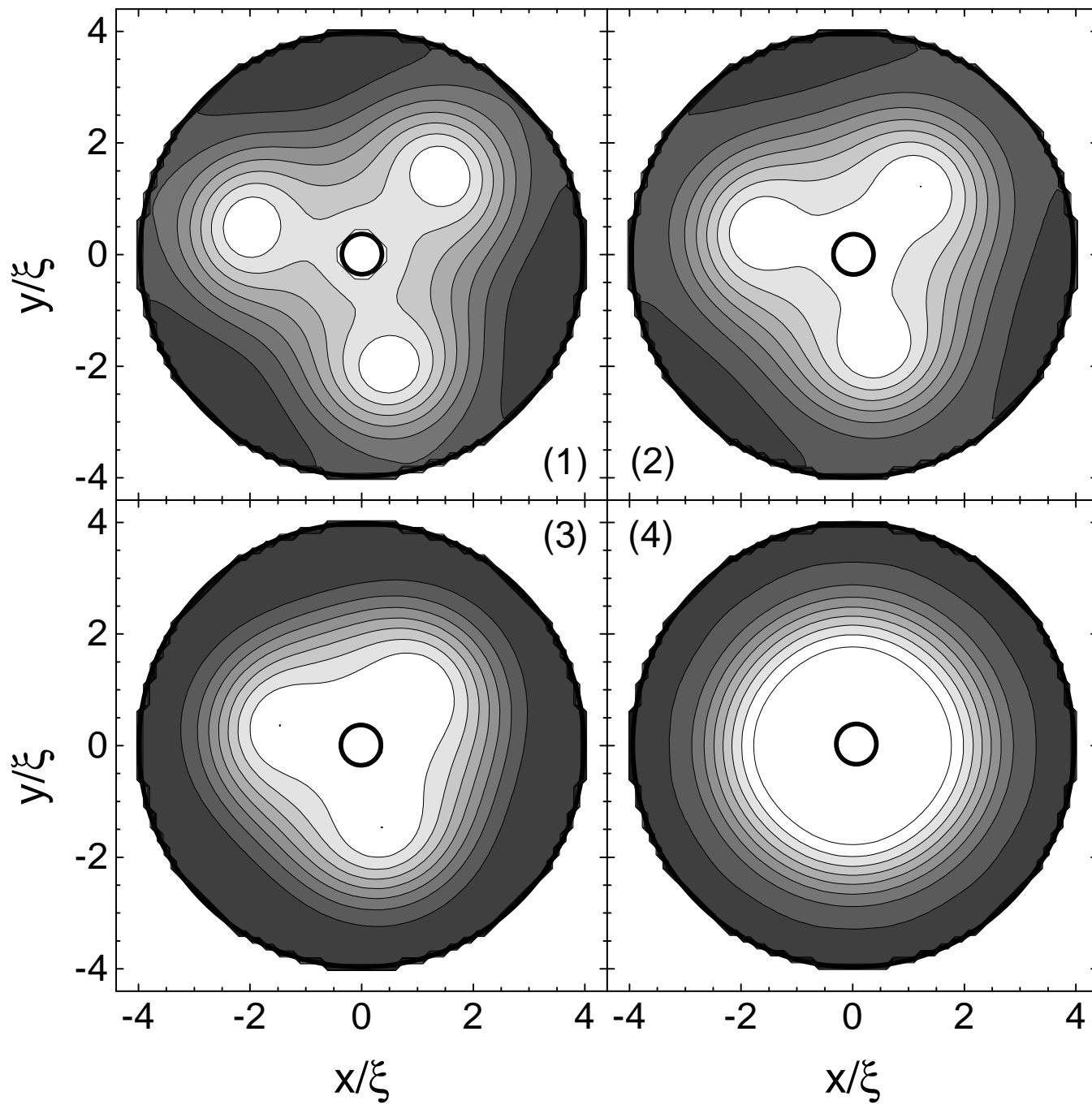
Fig. 9. The magnetic field range ($\Delta\phi = \pi R_o^2 \Delta H$) over which the L-state stays in the ground state for different values of the inner radius R_i and for outer radius (a) $R_o/\xi = 2$ and (b) $R_o/\xi = 4$. The horizontal dashed lines in (a) are for an increase with an integer number of flux quanta through an area with radius $\sqrt{R_i R_o}$.



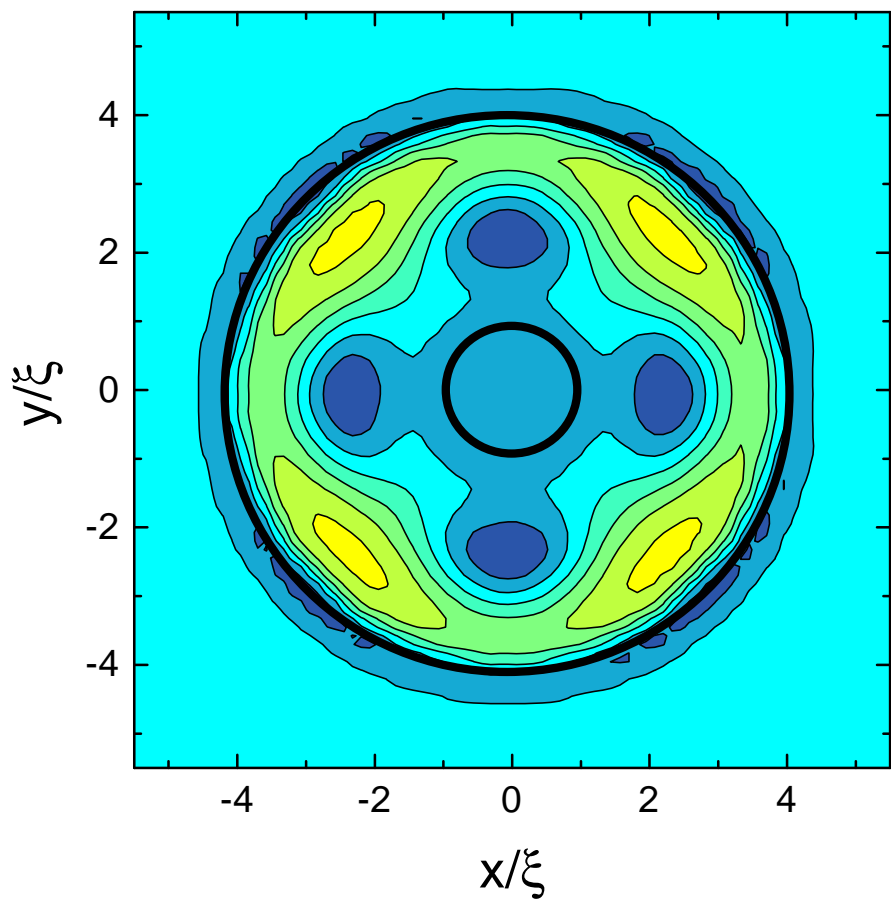








Magnetic field distribution



Phase φ ($\psi = |\psi| \exp(i\varphi)$)

